

Sparse Neural Additive Model: Interpretable Deep Learning with Feature Selection via Group Sparsity

Shiyun Xu* Zhiqi Bu† Pratik Chaudhari‡ Ian J. Barnett§

Abstract

Interpretable machine learning has demonstrated impressive performance while preserving explainability. In particular, neural additive models (NAM) offer the interpretability to the black-box deep learning and achieve state-of-the-art accuracy among the large family of generalized additive models. In order to empower NAM with feature selection and improve the generalization, we propose the sparse neural additive models (SNAM) that employ the group sparsity regularization (e.g. Group LASSO), where each feature is learned by a sub-network whose trainable parameters are clustered as a group. We study the theoretical properties for SNAM with novel techniques to tackle the non-parametric truth, thus extending from classical sparse linear models such as the LASSO, which only works on the parametric truth.

Specifically, we show that SNAM with subgradient and proximal gradient descents provably converges to zero training loss as $t \rightarrow \infty$, and that the estimation error of SNAM vanishes asymptotically as $n \rightarrow \infty$. We also prove that SNAM, similar to LASSO, can have exact support recovery, i.e. perfect feature selection, with appropriate regularization. Moreover, we show that the SNAM can generalize well and preserve the ‘identifiability’, recovering each feature’s effect. We validate our theories via extensive experiments and further testify to the good accuracy and efficiency of SNAM.

*Department of Applied Mathematics and Computational Science, University of Pennsylvania. Email: shiyunxu@sas.upenn.edu

†Department of Applied Mathematics and Computational Science, University of Pennsylvania.

‡Department of Electrical and Systems Engineering, University of Pennsylvania.

§Department of Biostatistics, Epidemiology, and Informatics, University of Pennsylvania.

1 Introduction

Deep learning has shown dominating performance on learning complex tasks, especially in high-stake domains such as finance, healthcare and criminal justice. However, most neural networks are not naturally as interpretable as decision trees or linear models. Even to answer fundamental questions like “what is the exact effect on the output if we perturb the input?”, neural networks oftentimes rely on complicated and ad-hoc methods to explain the model behavior, with additional training steps and loose theoretical guarantee. As a result, the black-box nature of neural networks renders difficult and risky for human to trust deep learning models or at least to understand them.

There is a long line of work studying the interpretable machine learning. At high level, existing methods can be categorized into two classes: (1) model-agnostic methods, and (2) innately interpretable models. On one hand, model-agnostic methods aim to explain the predictions of models that are innately black-box, via the feature importance and local approximation, which include Shapley values [Shapley, 2016, Strumbelj and Kononenko, 2014, Lundberg and Lee, 2017] and LIME [Ribeiro et al., 2016] as the representatives. On the other hand, directly interpretable models such as the decision-tree-based models and the generalized additive models (GAM), including the generalized linear models (GLM, [Nelder and Wedderburn, 1972]) as sub-cases, are the most widely applied and demonstrate amazing performance.

To give more details, GLM is a powerful family of models that relates a linear model with its response variable by a link function g .

$$g(\mathbb{E}(\mathbf{y})) = \beta + \sum_{j=1}^p \beta_j \mathbf{X}_j \quad (1)$$

where $\mathbf{y} \in \mathbb{R}^n$ is the response and \mathbf{X}_j is the j -th feature of the input matrix. However, such parametric form with β_j limits the capacity of GLM when

the unknown truth function takes a general and non-parametric form. This limitation motivates the development of GAM [Hastie and Tibshirani, 2017]:

$$g(\mathbb{E}(\mathbf{y})) = \beta + \sum_{j=1}^p f_j(\mathbf{X}_j) \equiv \beta + f(\mathbf{X}). \quad (2)$$

Here f_j is the unknown truth function (possibly non-linear) to be learned, which we refer to as the ‘effect’.

Recently, the neural additive model (NAM) [Agarwal et al., 2020] introduces a new member into the GAM family, which applies sub-networks to learn f_j effectively, making accurate predictions while preserving the explainable power. Similar to regular neural networks, NAM learns a non-parametric model (2) via its trainable parameters, instead of the functional approximation used by the traditional GAM. This parametric formulation allows NAM to be trained efficiently by off-the-shelf optimizers such as Adam. In addition, NAM can work flexibly with regression and classification problems, leveraging arbitrary network architecture to approximate f_j , hence fully exploiting the expressivity of deep learning.

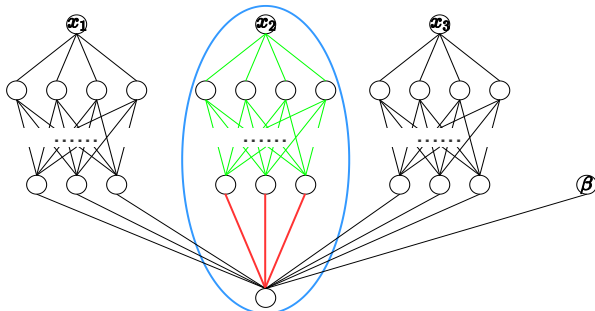


Figure 1: Architecture of NAM, with each sub-network (blue circle) being a group for Group LASSO regularization in SNAM. Note that in multi-class, multi-label, and multi-task problems, the last layer can have multiple neurons.

Yet, theoretical results about NAM on some important questions are missing: Does the convergence of NAM behave nicely? Does NAM guarantee to learn the true additive model consistently, as sample size increases? How to modify NAM such as to select features and whether the feature selection is accurate? Can we expect each sub-network in NAM to recover each f_j ?

In this paper, we answer these questions in the affirmative. We study the sparse NAM with specific

group sparsity regularization, especially the Group LASSO [Meier et al., 2008, Friedman et al., 2001], which reduces to NAM when the penalty is zero. We highlight that our SNAM is the first innately interpretable model that simultaneously uses neural networks and allows feature selection. Our contributions are as follows:

1. We propose an innately interpretable model – sparse neural additive model (SNAM) – to empower NAM with feature selection. In particular, SNAM can employ the Group LASSO penalty that regularizes each sub-network’s parameters as a group. Notice that LASSO is a special case of SNAM, when each sub-network has only one parameter. Our design easily extends to other SNAMs when we consider different group penalty such as the Group SLOPE.
2. We employ efficient and scalable optimizers, such as the subgradient and proximal methods (see Appendix B.1), to train SNAM. Consequently, we demonstrate its prediction power and trainability.
3. We establish an interesting connection between the LASSO and SNAM with Group LASSO regularization. Building on top of this, we rigorously derive the slow rate and the support recovery of SNAM. We show that SNAM approximates the true model, selects important features in a sample-efficient manner, and identifies individual functions f_j asymptotically.
4. We empirically validate our theoretical results via synthetic and real datasets, further illustrating that SNAM is trainable, accurate, effective in feature selection, and capable of effect identification. For example, SNAM can be 3 times faster than SPAM (see Table 2) and save roughly half of parameters in NAM, while preserving comparable performance (see Table 5).

For theoretical analysis, we focus on

$$\mathbf{y} = \sum_{j=1}^p f_j(\mathbf{X}_j) + \epsilon \quad (3)$$

where i.i.d. samples $\mathbf{X}_j \sim \mathcal{X}_j$ for $j \in [p]$ where \mathcal{X}_j is some distribution and the noise $\epsilon \sim SG(\sigma^2)$ where SG means sub-Gaussian with variance σ^2 . For algorithms and experiments, we extend to GAM in (2).

2 Additive Models in a Nutshell

Linear regression is one of the most classic model, on which various extensions are based. One extension is the LASSO [Tibshirani, 1996], a linear model that adds ℓ_1 penalty to the linear model. This penalty not only empowers ordinary linear regression with feature selection but also regularizes the model against overfitting. Another extension is the GLM, which adds a link function to relate the linear model with its response to work on more general problems (e.g. logistic regression for classification). Note that GLM can combine with the ℓ_1 penalty to give sparse logistic regression.

While GLMs are all additive and thus directly interpretable, GAMs further improve the capacity of models by introducing the non-linearity, for instance, in NAM [Agarwal et al., 2020] and Explainable Boosting Machines (EBM) [Lou et al., 2012, Nori et al., 2019]. In this work, we focus on NAM, a state-of-the-art GAM that incorporates neural networks and uses four types of regularization: dropout, weight decay (ℓ_2 penalty), output penalty, and feature dropout. Unfortunately, all these types of regularization do not enable feature selection for NAM.

Traditionally, one can only allow feature selection on GLMs (with ℓ_1 regularization) or a few special GAMs, e.g. sparse additive model (SPAM by Ravikumar et al. [2009], restated in Algorithm 1). As introduced in this paper, SNAM is a new member of GAM with feature selection. In addition, SNAM is the only GAM that is parametric (i.e. containing parameters that are trainable by gradient methods) besides GLMs: traditionally additive models are learned via the ‘backfitting algorithm’¹ [Breiman and Friedman, 1985], while neural networks are learned via gradient methods.

$$\boxed{\text{LASSO} \subseteq \text{GLM} \subseteq \text{NAM} \subseteq \text{SNAM} \subseteq \text{GAM}}$$

One drawback of the backfitting algorithm is that the computation time will increase linearly with the number of features. This is due to the asynchronous or sequential estimation for each feature and a lack of theoretical understanding from the convergence viewpoint. The other drawback is the heavy memory complexity when executing the ‘smoothing’ function (usually some smooth kernel splines) on large sample

¹The backfitting algorithm can be recovered from Algorithm 1 when $\lambda = 0$.

size. In fact, SNAM can out-speed SPAM by 3 times in Table 2 on synthetic datasets, and SPAM runs out of memory on all real datasets considered here.

We give a brief summary of additive models in Table 1.

Models	Non-linear model	Non-param truth	Parametric model	Feature selection
LASSO	No	No	Yes	Yes
GLM	No	No	Yes	Yes
EBM (Trees)	Yes	Yes	No	No
NAM	Yes	Yes	Yes	No
SPAM	Yes	Yes	No	Yes
SNAM	Yes	Yes	Yes	Yes

Table 1: Summary of additive (interpretable) models. In ‘Non-param truth’, Yes/No means whether a model works without assuming that the truth is parametric.

3 SNAM: Model and Optimization

3.1 Model and Linearization Regimes

To analyze SNAM under the regularization, for the j -th sub-network, we write the trainable parameters of as Θ_j (visualized in Figure 1 by the blue circle) and the output as h_j . Then we write the SNAM output as

$$h(\mathbf{X}, \Theta) = \sum_j h_j(\mathbf{X}_j, \Theta_j) + \beta$$

With these notations in place, we can learn the model via the following SNAM optimization problem with some group sparsity regularization and an arbitrary loss \mathcal{L} :

$$\min_{\Theta, \beta} \mathcal{L}(\mathbf{y}, \sum_j h_j(\mathbf{X}_j, \Theta_j) + \beta) + \text{GroupSparsity}(\{\Theta_j\}). \quad (4)$$

Notably, the group structure defined on sub-networks is the key to feature selection in SNAM: it explicitly penalizes Θ_j so that the entries in Θ_j are either all non-zero or all zero. The latter case happens when λ is large, resulting in the j -th feature to be not selected as $h_j = 0$.

In fact, if each sub-network has only a single parameter β_j and no hidden layers at all, then the Group LASSO penalty is equivalent to the LASSO penalty:

$\|\beta_j\|_2 = |\beta_j|$. Therefore, we view LASSO as the simplest version of SNAM with Group LASSO regularization. This connection leads to the theoretical findings in this work, since we will analyze the linearization of SNAM.

A long line of researches that linearizes the neural networks can be categorized into two main regimes: the neural tangent kernel (NTK) and the random feature (RF). The NTK regime linearizes the network under the ‘lazy training’ constraint, where $\Theta(t) \approx \Theta(0)$ during entire training process, by applying a first-order Taylor expansion at $\Theta(0)$. This lazy training phenomenon is usually guaranteed using the extremely (even infinitely) wide neural networks, and without any regularization² [Jacot et al., 2018, Xiao et al., 2020, Arora et al., 2019, Du et al., 2018, Allen-Zhu et al., 2019, Bu et al., 2021b, Zou et al., 2020]. Such limitation renders the NTK analysis invalid for SNAM.

The other branch of work uses the RF regime [Neal, 1996, Rahimi et al., 2007, Yehudai and Shamir, 2019, Ghorbani et al., 2021] to linearize the neural network by fixing the weights in all hidden layers after initialization, and only training the output layer’s weights. Mathematically, we decompose $\Theta_j = [\mathbf{w}_j, \theta_j]$. We denote \mathbf{w}_j as the weights of all hidden layers (green in Figure 1) and $\theta_j \in \mathbb{R}^m$ as the weights in the output layer (red in Figure 1). Then we can rewrite the output of SNAM as

$$\begin{aligned} h(\mathbf{X}, \mathbf{w}, \boldsymbol{\theta}) &= \sum_j h_j(\mathbf{X}_j, \mathbf{w}_j, \theta_j) + \beta \\ &= \sum_j g_j(\mathbf{X}_j, \mathbf{w}_j) \theta_j + \beta \end{aligned} \quad (5)$$

in which $\boldsymbol{\theta} := [\theta_1, \dots, \theta_p]$, $\mathbf{w} := [\mathbf{w}_1, \dots, \mathbf{w}_p]$, and the feature map $g_j : \mathbb{R} \rightarrow \mathbb{R}^m$ is the forward propagation of the j -th sub-network until the output layer.

In this RF regime, SNAM is linear in trainable parameters $\boldsymbol{\theta}$ (though non-linear in input \mathbf{X}) and is indeed a kernel regression, a topic with rich theoretical understanding.

3.2 Group Sparsity and Optimization Problems

It is well-known that group sparsity allows all parameters in the same group to be simultaneously non-zero or zero. One popular choice is the Group LASSO,

²Unfortunately, $\Theta(t)$ will be pushed away from its initialization $\Theta(0)$ towards zero even under weak regularization, breaking the lazy training assumption [Fang et al., 2021, Chen et al., 2020].

with which the SNAM problem becomes

$$\min_{\Theta, \beta} \mathcal{L}(\mathbf{y}, \sum_j h_j(\mathbf{X}_j, \Theta_j) + \beta) + \lambda \sum_j \|\Theta_j\|_2. \quad (6)$$

For another example, we may consider the Group SLOPE:

$$\min_{\Theta, \beta} \mathcal{L}(\mathbf{y}, \sum_j h_j(\mathbf{X}_j, \Theta_j) + \beta) + \sum_j \lambda_j \|\Theta_j\|_{2,(j)}, \quad (7)$$

where the penalty is a decreasing vector $(\lambda_1, \dots, \lambda_p)$ and $\|\Theta_j\|_{2,(j)}$ denotes the j -th largest element in $\{\|\Theta_1\|_2, \dots, \|\Theta_p\|_2\}$. We demonstrate other choices of group sparsity in Appendix B.2. In what follows, we focus on SNAM with the Group LASSO.

3.3 Random Feature SNAM

We study the RF neural network as a sub-class of SNAM, with two desirable benefits: (i) we do not restrict to weak (infinitesimal) regularization as in Wei et al. [2019]; (ii) we do not need neural networks to be wide. For the ease of presentation, we omit the output layer bias β :

$$h^{\text{RF}}(\mathbf{X}, \boldsymbol{\theta}) = \sum_{j=1}^p h_j^{\text{RF}}(\mathbf{X}_j, \theta_j) = \sum_{j=1}^p \mathbf{G}_j \theta_j$$

where the random features $\mathbf{G}_j := g_j(\mathbf{X}_j, \mathbf{w}(0)) \in \mathbb{R}^{n \times m}$. Therefore, the corresponding optimization for the RF network is

$$\hat{\boldsymbol{\theta}}^{\text{RF}} := \operatorname{argmin}_{\boldsymbol{\theta}} \mathcal{L}(\mathbf{y}, \mathbf{G}\boldsymbol{\theta}) + \lambda \sum_j \|\theta_j\|_2 \quad (8)$$

where $\mathbf{G} := [\mathbf{G}_1, \dots, \mathbf{G}_p]$ is the concatenation of \mathbf{G}_j .

3.4 Convergence of SNAM and RF

Algorithmically speaking, the general SNAM (4) can be efficiently optimized by existing optimizers, e.g. the subgradient methods [Shor, 2012, Boyd et al., 2003] and the proximal gradient descent (ProxGD) [Nittanda, 2014, Li and Lin, 2015, Parikh and Boyd, 2014] (c.f. Appendix B.1 for details), with possible acceleration (for example, subgradient Adam and Nesterov-accelerated ProxGD [Beck and Teboulle, 2009, Su et al., 2014]). In fact, we can show that the subgradient descent and ProxGD both provably find the minimizer of SNAM (4) and its RF variant (8).

Denoting Θ to denote all trainable parameters in SNAM and Θ_j as those in the j -th sub-network, we

claim both subgradient descent and ProxGD have the same gradient flow [Parikh and Boyd, 2014, Section 4.2]:

$$\frac{d\Theta}{dt} = -\frac{\partial(\mathcal{L}(\mathbf{y}, h(\mathbf{X}, \Theta)) + \lambda \sum_j \|\Theta_j\|_2)}{\partial\Theta}$$

Left multiply $\frac{\partial\Theta}{\partial t}^\top$ and integrate over time,

$$\int_0^\infty \left\| \frac{d\Theta}{dt} \right\|_2^2 dt = \int_0^\infty \frac{d(\mathcal{L}(t) + \lambda \sum_j \|\Theta_j(t)\|_2)}{dt} dt \leq \mathcal{L}(0) + \lambda \sum_j \|\Theta_j(0)\|_2.$$

Since the integral is increasing in time but upper bounded, we obtain that $\frac{d\Theta}{dt} \rightarrow 0$ and thus $\frac{d\mathcal{L}}{dt} \rightarrow 0$, i.e. \mathcal{L} converges to the minimum. The convergence result implies the trainability of SNAMs (and NAMs as a by-product when $\lambda = 0$) in practice.

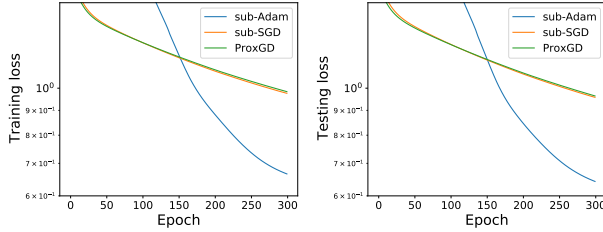


Figure 2: Loss convergence of SNAM on California Housing regression dataset, under different optimizers.

Henceforth, we focus on the RF SNAM minimizer $\hat{\theta}^{\text{RF}}$ in (3) and drop the super-script ‘RF’ for clearer presentation.

4 Non-Asymptotic Analysis of SNAM

In this section, we show that SNAM can approximate the truth model well on training set and achieve exact support recovery with finite number of samples.

We study the primal problem

$$\hat{\theta} := \operatorname{argmin}_{\theta} \frac{1}{2} \|\mathbf{y} - \sum_j \mathbf{G}_j \theta_j\|_2^2 + \lambda \sum_j \|\theta_j\|_2 \quad (9)$$

and equivalently the dual problem

$$\hat{\theta} := \operatorname{argmin}_{\theta: \sum_j \|\theta_j\|_2 \leq \frac{1}{2}} \frac{1}{2} \|\mathbf{y} - \sum_j \mathbf{G}_j \theta_j\|_2^2 \quad (10)$$

We point out that although the analysis of SNAM is similar to that of LASSO at high level, our analysis is technically more involved and requires novel tools, due to the fact that the true model (3) is non-parametric (unlike the LASSO whose true model is parametric).

4.1 Slow Rate with Group LASSO Penalty

Similar to the analysis of slow rate for the LASSO [Wainwright, 2009], our analysis needs SNAM to over-fit the training data under the low-dimensional \mathbf{G} regime.

Assumption 4.1 (Overfitting of SNAM). *Denoting the truth $\mathbf{f}_j := f_j(\mathbf{X}_j)$, we assume there exists μ such that*

$$\frac{1}{n} \|\mathbf{y} - \sum_j \mathbf{G}_j \hat{\theta}_j\|_2^2 \leq \frac{1}{n} \|\mathbf{y} - \sum_j \mathbf{f}_j\|_2^2 = \frac{1}{n} \|\epsilon\|_2^2.$$

To guarantee a unique solution of SNAM, we further assume that the SNAM feature map \mathbf{G} has full rank.

Assumption 4.2 (Full rank of feature map). $\mathbf{G} \in \mathbb{R}^{n \times M}$ has full column rank M and thus $\mathbf{G}^\top \mathbf{G} \in \mathbb{R}^{M \times M}$ is invertible.

Here M is the sum of numbers of neurons at the last hidden layer of each sub-network³. Our first result is the slow rate of the SNAM convergence $h(\mathbf{X}, \hat{\theta}) \rightarrow f(\mathbf{X})$ as $n \rightarrow \infty$. We highlight the definition of estimation error $\|f(\mathbf{X}) - h(\mathbf{X}, \hat{\theta})\|^2/n$, which is different from the prediction error $\|\mathbf{y} - h(\mathbf{X}, \hat{\theta})\|^2/n$.

Theorem 4.3. *Under Assumption 4.1 and Assumption 4.2, supposing $|f_j|$ is upper bounded by constant c_j and noise $\epsilon \sim SG(\sigma^2)$, then with probability at least $1 - \delta_1 - \delta_2$, we have for $\hat{\theta}$ in (10),*

$$\frac{1}{n} \left\| \sum_j (\mathbf{f}_j - \mathbf{G}_j \hat{\theta}_j) \right\|_2^2 \leq \frac{2\sigma}{\sqrt{n}} \left(\sum_j c_j / \sqrt{\delta_2} + \mu \max_j \sqrt{\mathbb{E} g_j(\mathcal{X}_j, \mathbf{w}_j(0))^2} \sqrt{2 \log(m_j / \delta_1)} \right)$$

where m_j is the width of output layer in the j -th sub-network and μ is the penalty coefficient.

³When all sub-networks have the same architecture, we write $M = mp$ where the last hidden layer width m . More generally, suppose the j -th sub-network has last hidden layer width m_j , then $M = \sum_j m_j$.

We refer the interested readers to Appendix A for the proof. In fact, we may further relax our assumption on the noise distribution in the true model (3), at the cost of a strictly worse bound for any δ_1 .

Corollary 4.4. *Under Assumption 4.1 and Assumption 4.2, supposing $|f_j|$ is upper bounded by constant c_j and noise has mean(ϵ) = 0, Var(ϵ) = σ^2 , then with probability at least $1 - \delta_1 - \delta_2$, we have for $\hat{\theta}$ in (10),*

$$\frac{1}{n} \left\| \sum_j (\mathbf{f}_j - \mathbf{G}_j \hat{\theta}_j) \right\|_2^2 \leq \frac{2\sigma}{\sqrt{n}} \left(\sum_j c_j / \sqrt{\delta_2} + \mu \max_j \sqrt{\mathbb{E}g_j(\mathcal{X}_j, \mathbf{w}_j(0))^2} \sqrt{m_j / \delta_1} \right)$$

The proof only needs slight modification by leveraging the Kolmogorov inequality instead of the maximal sub-Gaussian inequality in Theorem 4.3. In both Theorem 4.3 and Corollary 4.4, the MSE $\frac{1}{n} \left\| \sum_j (\mathbf{f}_j - \mathbf{G}_j \hat{\theta}_j) \right\|_2^2$ converges to zero with rate $1/\sqrt{n}$ as $n \rightarrow \infty$. We note that the convergence rate of SNAM has the same order as that of LASSO, but SNAM requires two probability quantities δ_1, δ_2 due to the non-parametric true model (3), whereas the LASSO only needs δ_1 .

4.2 Exact Support Recovery

There has been a long line of researches on the support recovery, particularly on the parametric models such as the LASSO [Bühlmann and Van De Geer, 2011, Wainwright, 2009, Tibshirani and Wasserman, 2017], where the support is defined on the parameters, e.g. $\text{supp}(\hat{\beta}) = \{j : \hat{\beta}_j \neq 0\}$, $\text{supp}(\beta) = \{j : \beta_j \neq 0\}$, and the regularization is also defined on the parameters via $\lambda \|\beta\|_1$. For non-parametric models like SPAM, the support is instead defined on the functions

$$S = \text{supp}(f) = \{j : f_j \neq 0\},$$

and the regularization is on the output function $\{h_j\}$. In contrast, our SNAM sets the sparse regularization on the parameters $\{\theta_j\}$, similar to LASSO. This explicit regularization allows us to borrow from the rich results of traditional support recovery for the LASSO and extend them to SNAM.

First, we assume that an insignificant feature ($j \notin S$) is small when regressing on the true features.

Assumption 4.5 (Mutual incoherence). *For some $\gamma > 0$, we have*

$$\left\| (\mathbf{G}_S^\top \mathbf{G}_S)^{-1} \mathbf{G}_S^\top \mathbf{G}_j \right\|_2 \leq 1 - \gamma, \text{ for } j \notin S \quad (11)$$

where \mathbf{G}_S is the concatenation of \mathbf{G}_j for all $j \in S$.

Next, we assume that the regularization is not too large to omit significant features.

Assumption 4.6 (Maximum regularization). *The Group LASSO penalty coefficient λ in (9) is small enough so that the following solution is dense*

$$\tilde{\theta}_S := \underset{\theta_S}{\text{argmin}} \frac{1}{2} \left\| \mathbf{y} - \sum_{j \in S} \mathbf{G}_j \theta_j \right\|_2^2 + \lambda \sum_{j \in S} \|\theta_j\|_2 \quad (12)$$

We define the support of any prediction function $h(\cdot; \hat{\theta})$ in two equivalent ways: one on the function and the other on the parameters,

$$\text{supp}(h) \equiv \{j : h_j \neq 0\} \equiv \{j : \|\hat{\theta}_j\|_2 \neq 0\}.$$

We prove in Appendix A that, with proper Group LASSO regularization, the SNAM recovers the true $\text{supp}(f)$ exactly.

Theorem 4.7. *Under Assumption 4.2, Assumption 4.5 and Assumption 4.6, then*

$$\lambda > \max_{j \notin S} \|\mathbf{G}_j^\top\|_\infty \|\mathbf{y}\|_\infty / \gamma$$

guarantees that the SNAM solution $\hat{\theta}$ in (9) has the exact support recovery, i.e. $\text{supp}(h) = \text{supp}(f)$.

5 Asymptotic Analysis of SNAM

In this section, we study the asymptotic consistency of SNAM and hence indicate its good generalization behavior. Our results build on top of the asymptotic zero loss between the ground truth and the prediction on training data, given by the slow rate in Theorem 4.3. The proofs can be found in Appendix A.

5.1 Consistency

We show in Theorem 5.1 that the SNAM h_n , when trained on n samples, converges to the unknown true model f in a probability measure. In other words, large amount of data promises that SNAM as a whole function can learn the truth.

Theorem 5.1. *Under the assumptions in Theorem 4.3, we have the convergence in probability measure:*

$$\lim_{n \rightarrow \infty} \rho(\{x \in \mathcal{X} : |f(x) - h_n(x)| \geq \varepsilon\}) = 0$$

for arbitrarily small $\epsilon > 0$. Here ρ is the probability measure of \mathcal{X} , the joint distribution of data \mathbf{X} . In words, the prediction function h_n converges to the true model f .

5.2 Effect Identifiability

Another more difficult challenge in the generalized additive models is the identifiability of individual effects, in the sense that we want to have $h_j \rightarrow f_j$ for all $j \in [p]$. Notice that since the identifiability is a stronger property than the consistency, we need to assume more about the feature distribution \mathcal{X}_j . We show that SNAM is capable of identifying the effects in Theorem 5.2.

Theorem 5.2 (Effect Identifiability). *Assuming $h_n \rightarrow f$ in probability measure of \mathcal{X} as $n \rightarrow \infty$, if \mathcal{X}_j is independent of \mathcal{X}_{-j} , then $\lim_{n \rightarrow \infty} h_{n,j}(x)$ converges to $f_j(x)$ in probability up to a constant.*

6 Experiments

In this section, we conduct multiple experiments on both synthetic and real datasets. we emphasize that here SNAM is not RF SNAM, i.e. we train all parameters in sub-networks. All experiments are conducted with one Tesla P100 GPU. We use MSE loss for regression, cross-entropy (CE) loss for classification, and wall-clock time for all tasks. Furthermore, we compare SNAM to other possibly sparse interpretable methods: NAM, ℓ_1 linear support vector machine (SVM), LASSO and SPAM [Ravikumar et al., 2009]. Experiment details such as data pre-processing, model architecture and hyperparameters are listed in Appendix D.

6.1 Synthetic Datasets

To validate our statistical analysis on SNAM, i.e. the feature selection (or support recovery), the estimation consistency and the effect identifiability, we experiment on synthetic regression and classification datasets. We emphasize that, it is necessary to work with synthetic data instead of real-world ones, since we need access to the truth f_j for our performance measures.

6.1.1 Data generation

We generate a data matrix $\mathbf{X} \in \mathbb{R}^{3000 \times 24}$ and denote the j -th column of \mathbf{X} as \mathbf{X}_j . \mathbf{y} is generated by the

following additive model, for regression and binary classification, respectively:

$$\begin{aligned} \mathbf{y} &= f_1(\mathbf{X}_1) + \dots + f_{24}(\mathbf{X}_{24}) + \mathcal{N}(0, 1), \\ \mathbb{P}(\mathbf{y} = 1) &= \text{sigmoid}(f_1(\mathbf{X}_1) + \dots + f_{24}(\mathbf{X}_{24})). \end{aligned}$$

where all f_j are zero functions except

$$\begin{aligned} f_1(\mathbf{X}_1) &= 2x^2 \tanh x \\ f_2(\mathbf{X}_2) &= \sin x \cos x + x^2 \\ f_3(\mathbf{X}_3) &= 20/(1 + e^{-5 \sin x}) \\ f_4(\mathbf{X}_4) &= 20 \sin^3 2x - 6 \cos x + x^2 \end{aligned}$$

6.1.2 Performance measures

Denote the output of each sub-network as \hat{f}_j . To illustrate the performance on the support recovery, we use precision and recall to compare \hat{f}_j and truth f_j . In particular, we use ℓ_2 norm of a sub-network’s weights to indicate whether $\hat{f}_j = 0$.

We now introduce the identification error (iden. error),

$$\begin{aligned} &\min_{c_j \in \mathbb{R}} \frac{1}{n} \|\hat{f}_j(\mathbf{X}_j) - f_j(\mathbf{X}_j) - c_j\|_2^2 \\ &= \frac{1}{n} \|\hat{f}_j(\mathbf{X}_j) - f_j(\mathbf{X}_j) - \hat{c}_j\|_2^2 \end{aligned}$$

in which $\hat{c}_j := \frac{1}{n} \sum_{i=1}^n (\hat{f}_j(\mathbf{X}_{ij}) - f_j(\mathbf{X}_{ij}))$. Notice that Theorem 5.2 claims the convergence up to a constant \hat{c}_j .

6.1.3 Results

	ℓ_1 SVM	LASSO	SPAM	SNAM
MSE loss	140.7	139.7	25.75	10.61
Precision	0.17	1.00	0.17	1.00
Recall	1.00	1.00	1.00	1.00
Iden. error	5.90	6.09	3.07	0.69
Time (sec)	0.005	0.007	152.1	48.52
#. Feature	24	4	4	4
#. Param	24	4	-	127201

Table 2: Performance of sparse interpretable methods on synthetic regression.

In Table 2, for regression task, SNAM dominates existing sparse interpretable methods in all measures. Especially, SNAM (which includes LASSO as a sub-case) is the only method that achieves exact support recovery, obtaining perfect precision and recall scores.

When facing complicated target functions, SNAM, as a non-linear model, significantly outperforms linear models like linear SVM and LASSO, in terms of test loss and identification error. In contrast to SPAM, another non-linear model that achieves low loss, SNAM outperforms in both loss and efficiency, with a 3 times speed-up. We further visualize the effects learned by SNAM in Figure 3, demonstrating the strong approximation offered by the neural networks, and leave those learned by other interpretable methods in Appendix C.

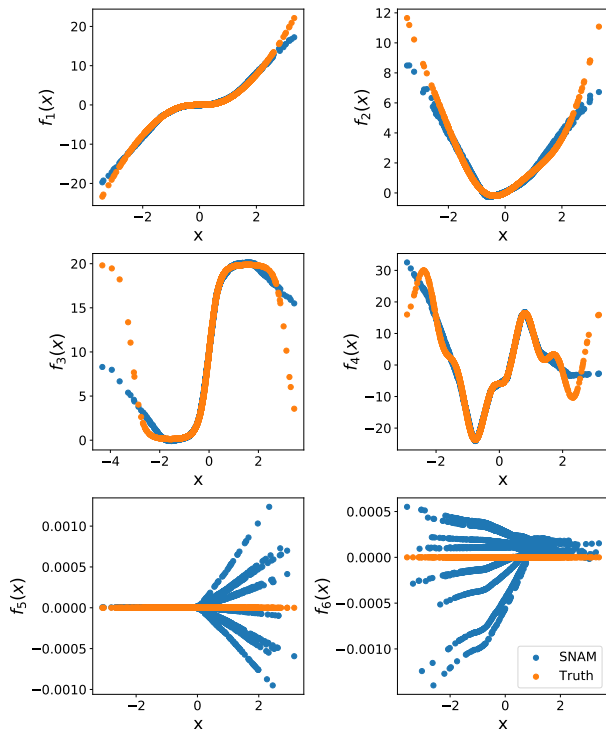


Figure 3: Individual effect learned by SNAM on synthetic regression. Blue dots are prediction $\hat{f}_j(\mathbf{X}_j)$ and orange dots are truth $f_j(\mathbf{X}_j)$, with $j = 1, \dots, 6$.

Similarly in Table 3, for classification task, SNAM again significantly outperforms existing sparse interpretable methods: roughly 20% higher accuracy and 33% higher precision. Here LASSO means ℓ_1 regularized logistic regression and SPAM cannot perform the classification in original text [Ravikumar et al., 2009].

6.2 California Housing Regression

California Housing [Pace and Barry, 1997] is a dataset for studying the effect of community characteristics

	ℓ_1 SVM	LASSO	SPAM	SNAM
CE loss	0.27	0.26	-	0.15
Test accuracy	73.2	74.2	-	94.1
Precision	0.57	0.67	-	1.00
Recall	1.00	1.00	-	1.00
Time (sec)	0.005	0.019	-	10.10
#. Feature	13	6	-	4
#. Param	13	6	-	128402

Table 3: Performance of sparse interpretable methods on synthetic classification.

on housing prices in California districts from 1990 U.S. census. The task is to predict the median housing price based on 20640 examples and 8 features. In Agarwal et al. [2020], a well-trained NAM deems the median income, latitude and longitude as the most significant features for an accurate prediction. Reassuringly, our SNAM concurs with their conclusion by selecting the same features. Although the conclusion is the same, we highlight a key difference between the approaches: while the authors in Agarwal et al. [2020] base their conclusion on the ad-hoc visual examination of the shape function \hat{f}_j , our approach is based on a hypothesis testing: $\theta_j = 0$ v.s. $\theta_j \neq 0$ where θ_j is all parameters in a sub-network. We recognize a small decrease in the loss as the cost of feature selection, when compared to NAM, but SNAM can save 12.5% in the number of parameters (or memory). Additionally, SNAM still outperforms other sparse interpretable methods. In fact, although SNAM takes longer to achieve its optimal performance in Section 6.2, it only takes about 14 seconds to outperform the optimal LASSO and SVM.

	ℓ_1 SVM	LASSO	NAM	SNAM
MSE loss	0.654	0.712	0.451	0.567
MAE loss	0.594	0.654	0.479	0.526
R^2 score	0.501	0.457	0.696	0.645
Time (sec)	1.37	0.01	343	340
#. Feature	6	2	8	7
#. Param	6	2	42401	37101

Table 4: Performance of interpretable methods on California Housing dataset.

6.3 COMPAS Classification

COMPAS is a widely used commercial tool to predict the recidivism risk based on defendants' features and

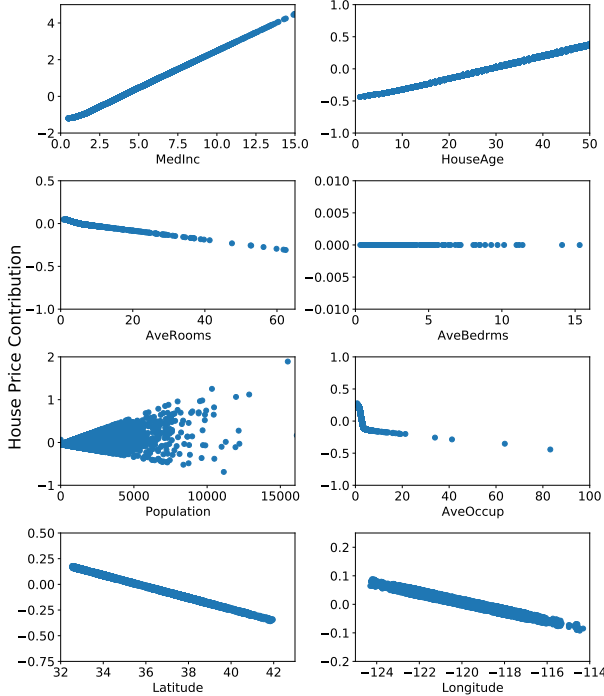


Figure 4: Individual effect learned by SNAM on California Housing dataset.

it is known for its racial bias against the black defendants. The ProPublica released the recidivism dataset [Angwin et al., 2016], that includes the characteristics of defendants in Broward County, Florida, and the predictions on reoffending by the COMPAS algorithm. This dataset has 6172 examples and 13 features ⁴.

	ℓ_1 SVM	LASSO	NAM	SNAM
CE loss	0.486	0.484	0.503	0.504
Test accuracy	75.3	75.4	75.3	75.6
AUC score	0.744	0.743	0.714	0.745
Time (sec)	0.106	0.175	27.5	27.4
#. Feature	13	12	13	5
#. Param	13	12	69552	26750

Table 5: Performance of interpretable methods on COMPAS dataset.

In Table 5, we notice that all interpretable methods perform similarly, and SNAM has the highest AUC score between label and prediction, even though it only contains 54% of NAM’s parameters. A closer

⁴The data preprocessing follows <https://github.com/propublica/compas-analysis>.

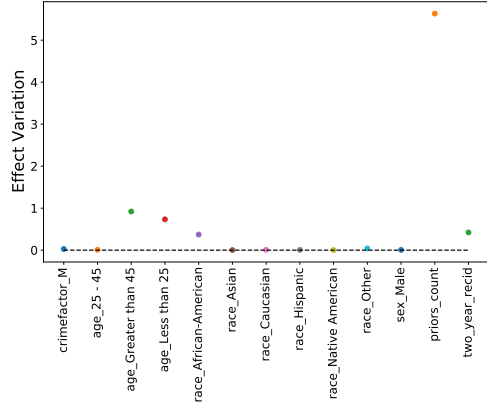


Figure 5: Variation of effects learned by SNAM on COMPAS dataset.

look at Figure 5 describes the relations between features and the variation of effect, which is gap between the minimum recidivism risk and the maximum one among all individual samples for a particular feature, i.e. $\max_i \hat{f}_j(X_{ij}) - \min_i \hat{f}_j(X_{ij})$. If the variation of an effect is large, then SNAM indicates the feature is significant. Indeed, the top 5 features selected by SNAM are prior counts, ages, two year recidivism and whether the defendant is African American. The last feature clearly demonstrates SNAM’s explainability of the COMPAS algorithm’s racial bias. In short, the features selected by SNAM are consistent with NAM’s selection based on shape functions (c.f. Appendix C).

6.4 Super-conductivity Regression

We further experiment on the super-conductivity dataset from UCI repository, aiming to predict the critical temperature of super-conductors based on physical quantities (e.g. atomic radius, mass, density...) and chemical formulae. We highlight that the Super-conductivity is a high-dimensional dataset with 21263 samples and 131 features⁵, whereas all datasets in Agarwal et al. [2020] have at most 30 features.

We note that SNAM obtains similar performance as NAM and LASSO. In addition, the sparsity in SNAM saves 45% number of parameters. In fact, given that NAM gives the best performance, a practitioner can always choose small penalty in SNAM in order to trade model efficiency for better performance.

⁵The original dataset has 168 features. We remove the column `material` and all columns with variance less than 5%.

	ℓ_1 SVM	LASSO	NAM	SNAM
MSE loss	410.0	311.7	274.1	280.3
MAE loss	15.47	13.43	11.56	12.09
R^2 score loss	0.654	0.731	0.787	0.775
Time (sec)	5.00	1.87	682	688
#. Feature	100	50	131	72
#. Param	100	50	6289	3457

Table 6: Performance of interpretable methods on super-conductivity dataset.

7 Discussion

In this work, we propose the sparse neural additive model (SNAM) which applies a specific Group LASSO regularization explicitly to NAM. On one hand, SNAM is an interpretable deep learning model where the effect of each feature on the output can be extracted. On the other hand, the Group LASSO regularization empowers the network to select informative features, in the same way that LASSO empowers the linear model. We develop theoretical analysis of the optimization, the slow rate, the support recovery, the consistency of prediction, and the effect identifiability. Additionally, our experiments demonstrate the advantage of SNAM in memory and training efficiency, especially over non-regularized NAM and existing regularized interpretable methods. However, the superiority in performance usually comes at the price of longer training time than simpler methods like LASSO.

For future directions, one may further extend SNAM’s theory to the fast convergence rate [Van De Geer and Bühlmann, 2009] in sample size, or to the jointly trained SNAM in terms of time. We believe the theoretical analysis and empirical evaluation can be explored for a whole family of interesting SNAMs. For example, while SNAM with Group LASSO penalty contains LASSO as sub-case, we can view SNAM with Group SLOPE [Brzyski et al., 2019] penalty as extension of SLOPE [Bogdan et al., 2015]. Other possible extensions of elastic net [Zou and Hastie, 2005], adaptive LASSO [Zou, 2006], K -level SLOPE [Zhang and Bu, 2021, Bu et al., 2021a] are also possible with SNAM (see Appendix B.2 for examples).

References

Rishabh Agarwal, Nicholas Frosst, Xuezhou Zhang, Rich Caruana, and Geoffrey E Hinton. Neural additive models: Interpretable machine learning

with neural nets. *arXiv preprint arXiv:2004.13912*, 2020.

Zeyuan Allen-Zhu, Yuanzhi Li, and Zhao Song. A convergence theory for deep learning via overparameterization. In *International Conference on Machine Learning*, pages 242–252. PMLR, 2019.

Julia Angwin, Jeff Larson, Surya Mattu, and Lauren Kirchner. Machine bias. *propublica*, may 23, 2016, 2016.

Sanjeev Arora, Simon S Du, Wei Hu, Zhiyuan Li, Ruslan Salakhutdinov, and Ruosong Wang. On exact computation with an infinitely wide neural net. *arXiv preprint arXiv:1904.11955*, 2019.

Amir Beck and Marc Teboulle. A fast iterative shrinkage-thresholding algorithm for linear inverse problems. *SIAM journal on imaging sciences*, 2(1): 183–202, 2009.

Małgorzata Bogdan, Ewout Van Den Berg, Chiara Sabatti, Weijie Su, and Emmanuel J Candès. Slope—adaptive variable selection via convex optimization. *The annals of applied statistics*, 9(3): 1103, 2015.

Stéphane Boucheron, Gábor Lugosi, and Pascal Massart. *Concentration inequalities: A nonasymptotic theory of independence*. Oxford university press, 2013.

Stephen Boyd, Lin Xiao, and Almir Mutapcic. Subgradient methods. *lecture notes of EE392o, Stanford University, Autumn Quarter, 2004:2004–2005*, 2003.

Leo Breiman and Jerome H Friedman. Estimating optimal transformations for multiple regression and correlation. *Journal of the American Statistical Association*, 80(391):580–598, 1985.

Damian Brzyski, Alexej Gossmann, Weijie Su, and Małgorzata Bogdan. Group slope—adaptive selection of groups of predictors. *Journal of the American Statistical Association*, 114(525):419–433, 2019.

Zhiqi Bu, Jason Klusowski, Cynthia Rush, and Weijie J Su. Characterizing the slope trade-off: A variational perspective and the donoho-tanner limit. *arXiv preprint arXiv:2105.13302*, 2021a.

Zhiqi Bu, Shiyun Xu, and Kan Chen. A dynamical view on optimization algorithms of overparameterized neural networks. In *International Conference on Artificial Intelligence and Statistics*, pages 3187–3195. PMLR, 2021b.

- Peter Bühlmann and Sara Van De Geer. *Statistics for high-dimensional data: methods, theory and applications*. Springer Science & Business Media, 2011.
- Zixiang Chen, Yuan Cao, Quanquan Gu, and Tong Zhang. A generalized neural tangent kernel analysis for two-layer neural networks. In H. Larochelle, M. Ranzato, R. Hadsell, M. F. Balcan, and H. Lin, editors, *Advances in Neural Information Processing Systems*, volume 33, pages 13363–13373. Curran Associates, Inc., 2020. URL <https://proceedings.neurips.cc/paper/2020/file/9afe487de556e59e6db6c862adfe25a4-Paper.pdf>.
- Simon S Du, Xiyu Zhai, Barnabas Poczos, and Aarti Singh. Gradient descent provably optimizes overparameterized neural networks. *arXiv preprint arXiv:1810.02054*, 2018.
- Rick Durrett. *Probability: theory and examples*, volume 49. Cambridge university press, 2019.
- Cong Fang, Hanze Dong, and Tong Zhang. Mathematical models of overparameterized neural networks. *Proceedings of the IEEE*, 109(5):683–703, 2021.
- Jerome Friedman, Trevor Hastie, Robert Tibshirani, et al. *The elements of statistical learning*, volume 1. Springer series in statistics New York, 2001.
- Behrooz Ghorbani, Song Mei, Theodor Misiakiewicz, and Andrea Montanari. Linearized two-layers neural networks in high dimension. *The Annals of Statistics*, 49(2):1029–1054, 2021.
- Trevor J Hastie and Robert J Tibshirani. *Generalized additive models*. Routledge, 2017.
- Arthur Jacot, Franck Gabriel, and Clément Hongler. Neural tangent kernel: Convergence and generalization in neural networks. *arXiv preprint arXiv:1806.07572*, 2018.
- Huan Li and Zhouchen Lin. Accelerated proximal gradient methods for nonconvex programming. *Advances in neural information processing systems*, 28: 379–387, 2015.
- Yin Lou, Rich Caruana, and Johannes Gehrke. Intelligible models for classification and regression. In *Proceedings of the 18th ACM SIGKDD international conference on Knowledge discovery and data mining*, pages 150–158, 2012.
- Scott M Lundberg and Su-In Lee. A unified approach to interpreting model predictions. In *Proceedings of the 31st international conference on neural information processing systems*, pages 4768–4777, 2017.
- Lukas Meier, Sara Van De Geer, and Peter Bühlmann. The group lasso for logistic regression. *Journal of the Royal Statistical Society: Series B (Statistical Methodology)*, 70(1):53–71, 2008.
- Radford M Neal. Priors for infinite networks. In *Bayesian Learning for Neural Networks*, pages 29–53. Springer, 1996.
- John Ashworth Nelder and Robert WM Wedderburn. Generalized linear models. *Journal of the Royal Statistical Society: Series A (General)*, 135(3):370–384, 1972.
- Atsushi Nitanda. Stochastic proximal gradient descent with acceleration techniques. *Advances in Neural Information Processing Systems*, 27:1574–1582, 2014.
- Harsha Nori, Samuel Jenkins, Paul Koch, and Rich Caruana. Interpretml: A unified framework for machine learning interpretability. *arXiv preprint arXiv:1909.09223*, 2019.
- R Kelley Pace and Ronald Barry. Sparse spatial autoregressions. *Statistics & Probability Letters*, 33(3):291–297, 1997.
- Neal Parikh and Stephen Boyd. Proximal algorithms. *Foundations and Trends in optimization*, 1(3):127–239, 2014.
- Ali Rahimi, Benjamin Recht, et al. Random features for large-scale kernel machines. In *NIPS*, volume 3, page 5. Citeseer, 2007.
- Pradeep Ravikumar, John Lafferty, Han Liu, and Larry Wasserman. Sparse additive models. *Journal of the Royal Statistical Society: Series B (Statistical Methodology)*, 71(5):1009–1030, 2009.
- Marco Tulio Ribeiro, Sameer Singh, and Carlos Guestrin. ” why should i trust you?” explaining the predictions of any classifier. In *Proceedings of the 22nd ACM SIGKDD international conference on knowledge discovery and data mining*, pages 1135–1144, 2016.
- Lloyd S Shapley. *17. A value for n-person games*. Princeton University Press, 2016.

- Naum Zuselevich Shor. *Minimization methods for non-differentiable functions*, volume 3. Springer Science & Business Media, 2012.
- Erik Strumbelj and Igor Kononenko. Explaining prediction models and individual predictions with feature contributions. *Knowledge and information systems*, 41(3):647–665, 2014.
- Weijie Su, Stephen Boyd, and Emmanuel Candes. A differential equation for modeling nesterov’s accelerated gradient method: Theory and insights. *Advances in neural information processing systems*, 27:2510–2518, 2014.
- Robert Tibshirani. Regression shrinkage and selection via the lasso. *Journal of the Royal Statistical Society: Series B (Methodological)*, 58(1):267–288, 1996.
- Ryan Tibshirani and Larry Wasserman. Sparsity, the lasso, and friends. *Lecture notes from “Statistical Machine Learning,” Carnegie Mellon University, Spring*, 2017.
- Sara A Van De Geer and Peter Bühlmann. On the conditions used to prove oracle results for the lasso. *Electronic Journal of Statistics*, 3:1360–1392, 2009.
- Martin J Wainwright. Sharp thresholds for high-dimensional and noisy sparsity recovery using ℓ_1 -constrained quadratic programming (lasso). *IEEE transactions on information theory*, 55(5):2183–2202, 2009.
- Colin Wei, Jason Lee, Qiang Liu, and Tengyu Ma. Regularization matters: Generalization and optimization of neural nets vs their induced kernel. 2019.
- Lechao Xiao, Jeffrey Pennington, and Samuel Schoenholz. Disentangling trainability and generalization in deep neural networks. In *International Conference on Machine Learning*, pages 10462–10472. PMLR, 2020.
- Gilad Yehudai and Ohad Shamir. On the power and limitations of random features for understanding neural networks. *Advances in Neural Information Processing Systems*, 32:6598–6608, 2019.
- Yiliang Zhang and Zhiqi Bu. Efficient designs of slope penalty sequences in finite dimension. In *International Conference on Artificial Intelligence and Statistics*, pages 3277–3285. PMLR, 2021.
- Difan Zou, Yuan Cao, Dongruo Zhou, and Quanquan Gu. Gradient descent optimizes over-parameterized deep relu networks. *Machine Learning*, 109(3):467–492, 2020.
- Hui Zou. The adaptive lasso and its oracle properties. *Journal of the American statistical association*, 101(476):1418–1429, 2006.
- Hui Zou and Trevor Hastie. Regularization and variable selection via the elastic net. *Journal of the royal statistical society: series B (statistical methodology)*, 67(2):301–320, 2005.

A Proofs of Main Results

A.1 Proof of Theorem 4.3

Proof. By the Lagrange duality, for any penalty $\lambda > 0$, there exists some $\mu > 0$ such that the optimization problem

$$\min_{\boldsymbol{\theta}} \frac{1}{2} \|\mathbf{y} - \sum_j \mathbf{G}_j \boldsymbol{\theta}_j\|_2^2 + \lambda \sum_j \|\boldsymbol{\theta}_j\|_2$$

is equivalent to

$$\min_{\boldsymbol{\theta}} \frac{1}{2} \|\mathbf{y} - \sum_j \mathbf{G}_j \boldsymbol{\theta}_j\|_2^2 \quad \text{s.t.} \quad \sum_j \|\boldsymbol{\theta}_j\|_2 \leq \mu$$

From Assumption 4.1, the minimizer $\hat{\boldsymbol{\theta}}$ satisfies that

$$\frac{1}{n} \|\boldsymbol{\epsilon} + \sum_j (\mathbf{f}_j - \mathbf{G}_j \hat{\boldsymbol{\theta}}_j)\|_2^2 = \frac{1}{n} \|\mathbf{y} - \sum_j \mathbf{G}_j \hat{\boldsymbol{\theta}}_j\|_2^2 \leq \frac{1}{n} \|\mathbf{y} - \sum_j \mathbf{f}_j\|_2^2 = \frac{1}{n} \|\boldsymbol{\epsilon}\|_2^2. \quad (13)$$

Expanding the left-most term,

$$\frac{1}{n} \|\boldsymbol{\epsilon} + \sum_j (\mathbf{f}_j - \mathbf{G}_j \hat{\boldsymbol{\theta}}_j)\|_2^2 = \frac{1}{n} \|\boldsymbol{\epsilon}\|_2^2 + \frac{1}{n} \left\| \sum_j (\mathbf{f}_j - \mathbf{G}_j \hat{\boldsymbol{\theta}}_j) \right\|_2^2 + \frac{2}{n} \left\langle \boldsymbol{\epsilon}, \sum_j (\mathbf{f}_j - \mathbf{G}_j \hat{\boldsymbol{\theta}}_j) \right\rangle$$

Substituting back to (13) and after some rearranging, we get:

$$\begin{aligned} \frac{1}{n} \left\| \sum_j (\mathbf{f}_j - \mathbf{G}_j \hat{\boldsymbol{\theta}}_j) \right\|_2^2 &\leq \frac{2}{n} \sum_j \left\langle \boldsymbol{\epsilon}, \mathbf{G}_j \hat{\boldsymbol{\theta}}_j - \mathbf{f}_j \right\rangle \\ &\leq \frac{2}{n} \sum_j \left| \boldsymbol{\epsilon}^\top (\mathbf{G}_j \hat{\boldsymbol{\theta}}_j - \mathbf{f}_j) \right| \\ &\leq \frac{2}{n} \sum_j (|\boldsymbol{\epsilon}^\top \mathbf{G}_j \hat{\boldsymbol{\theta}}_j| + |\boldsymbol{\epsilon}^\top \mathbf{f}_j|) \\ &\leq \frac{2}{n} \sum_j (\|\boldsymbol{\epsilon}^\top \mathbf{G}_j \hat{\boldsymbol{\theta}}_j\|_2 + \|\boldsymbol{\epsilon}^\top \mathbf{f}_j\|_2) \\ &\leq \frac{2}{n} \left(\sum_j \|\mathbf{G}_j^\top \boldsymbol{\epsilon}\|_\infty \|\hat{\boldsymbol{\theta}}_j\|_2 + \sum_j \|\mathbf{f}_j\|_\infty \|\boldsymbol{\epsilon}\|_2 \right) \\ &\leq \frac{2}{n} \left(\sum_j \|\mathbf{G}_j^\top \boldsymbol{\epsilon}\|_\infty \|\hat{\boldsymbol{\theta}}_j\|_2 + \sum_j c_j \|\boldsymbol{\epsilon}\|_2 \right) \end{aligned}$$

where the third inequality follows by the triangular inequality and the second last inequality holds by the Holder's inequality. Note that $\|\mathbf{G}_j^\top \boldsymbol{\epsilon}\|_\infty = \max_{k=1,2,\dots,m} |(\mathbf{G}_j^\top)_k \boldsymbol{\epsilon}|$ is a maximum of m Gaussians. Here $(\mathbf{G}_j^\top)_k \boldsymbol{\epsilon} \in \mathbb{R}^n$ is the k -th feature fed into the output layer of the j -th sub-network. For each k , $(\mathbf{G}_j^\top)_k \boldsymbol{\epsilon}$ has mean zero and variance

$$\text{Var}((\mathbf{G}_j^\top)_k \boldsymbol{\epsilon}) = \sigma^2 \mathbb{E}((\mathbf{G}_j^\top)_k (\mathbf{G}_j)_k) = n \sigma^2 \mathbb{E}g_j(\mathcal{X}_j, \mathbf{w}_j(0))^2$$

By the maximal sub-Gaussian inequality Boucheron et al. [2013], for any $\delta_1 > 0$, with probability at least $1 - \delta_1$:

$$\|\mathbf{G}_j^\top \boldsymbol{\epsilon}\|_\infty = \max_{k=1,2,\dots,m} |(\mathbf{G}_j)_k \boldsymbol{\epsilon}| \leq \sigma \sqrt{n \mathbb{E}g_j(\mathcal{X}_j, \mathbf{w}_j(0))^2} \sqrt{2 \log(m_j/\delta_1)}.$$

Furthermore, by Markov's inequality, with probability at least $1 - \delta_2$, we have $\|\boldsymbol{\epsilon}\|_2^2 \leq \mathbb{E}(\|\boldsymbol{\epsilon}\|_2^2)/\delta_2 = n\sigma^2/\delta_2$. In summary, we obtain

$$\begin{aligned}
& \frac{1}{n} \left\| \sum_j (\mathbf{f}_j - \mathbf{G}_j \hat{\boldsymbol{\theta}}_j) \right\|_2^2 \\
& \leq \frac{2}{n} \left(\sum_j \|\mathbf{G}_j^\top \boldsymbol{\epsilon}\|_\infty \|\hat{\boldsymbol{\theta}}_j\|_2 + \sum_j c_j \|\boldsymbol{\epsilon}\|_2 \right) \\
& \leq \frac{2}{\sqrt{n}} \left(\sum_j \sigma \sqrt{\mathbb{E}g_j(\mathcal{X}_j, \mathbf{w}_j(0))^2} \sqrt{2 \log(m_j/\delta_1)} \|\hat{\boldsymbol{\theta}}_j\|_2 + \sum_j c_j \sigma / \sqrt{\delta_2} \right) \\
& \leq \frac{2\sigma}{\sqrt{n}} \left(\mu \max_j \sqrt{\mathbb{E}g_j(\mathcal{X}_j, \mathbf{w}_j(0))^2} \sqrt{2 \log(m_j/\delta_1)} + \sum_j c_j / \sqrt{\delta_2} \right)
\end{aligned}$$

□

A.2 Proof of Theorem 4.7

For ease of presentation, we assume each sub-network has the same architecture, with last layer width m .

Proof. We construct and study a specific vector $\tilde{\boldsymbol{\theta}} \in \mathbb{R}^{|S|m \times 1}$ by setting $\tilde{\boldsymbol{\theta}}_S$ as in (12) and $\tilde{\boldsymbol{\theta}}_j = \mathbf{0}$ for $j \notin S$: denoting the complement set of S as S^C , we have:

$$\tilde{\boldsymbol{\theta}}_S = \operatorname{argmin}_{\boldsymbol{\theta}_S} \frac{1}{2} \left\| \mathbf{y} - \sum_{j \in S} \mathbf{G}_j \boldsymbol{\theta}_j \right\|_2^2 + \lambda \sum_{j \in S} \|\boldsymbol{\theta}_j\|_2 \quad \text{and} \quad \tilde{\boldsymbol{\theta}}_{S^C} = \mathbf{0}.$$

From Assumption 4.6 (maximum regularization), we have that $\tilde{\boldsymbol{\theta}}_S$ is dense, i.e. $\tilde{\boldsymbol{\theta}}_j \neq \mathbf{0}$ for all $j \in S$. Therefore, if the constructed $\tilde{\boldsymbol{\theta}}$ is indeed the SNAM solution $\hat{\boldsymbol{\theta}}$ in (9), then $\operatorname{supp}(h) \supseteq \operatorname{supp}(f)$. Further, $\tilde{\boldsymbol{\theta}}_{S^C} = \mathbf{0}$ leads to $\operatorname{supp}(h) = S = \operatorname{supp}(f)$.

Next, we check that the constructed $\tilde{\boldsymbol{\theta}}$ is indeed the solution of SNAM in (9) via the KKT condition, which requires that for all $j \in [p]$,

$$\mathbf{G}_j^\top \left(\sum_{l=1}^p \mathbf{G}_l \tilde{\boldsymbol{\theta}}_l - \mathbf{y} \right) + \lambda \mathbf{s}_j = \mathbf{G}_j^\top (\mathbf{G}_S \tilde{\boldsymbol{\theta}}_S - \mathbf{y}) + \lambda \mathbf{s}_j = 0 \tag{14}$$

Here \mathbf{s}_j is the subgradient of $\|\tilde{\boldsymbol{\theta}}_j\|_2$, which is $\tilde{\boldsymbol{\theta}}_j / \|\tilde{\boldsymbol{\theta}}_j\|_2$ if $\tilde{\boldsymbol{\theta}}_j \neq \mathbf{0}$ and otherwise within a unit sphere. The first equality of (14) follows by the construction $\tilde{\boldsymbol{\theta}}_{S^C} = \mathbf{0}$. We break (14) into the support set S and its complement S^C ,

$$\mathbf{G}_S^\top (\mathbf{y} - \mathbf{G}_S \tilde{\boldsymbol{\theta}}_S) = \lambda \mathbf{s}_S \tag{15}$$

$$\mathbf{G}_{S^C}^\top (\mathbf{y} - \mathbf{G}_S \tilde{\boldsymbol{\theta}}_S) = \lambda \mathbf{s}_{S^C} \tag{16}$$

Notice that if both KKT conditions (15) and (16) are satisfied by $\tilde{\boldsymbol{\theta}}$, then $\tilde{\boldsymbol{\theta}} = \hat{\boldsymbol{\theta}}$. For $j \in S$, the KKT condition in (15) is the same as that of (12) and hence satisfied by the definition of $\tilde{\boldsymbol{\theta}}_S$. For $j \notin S$, our goal is to show $\|\mathbf{s}_j\|_2 < 1$, which is a sufficient condition to guarantee $\tilde{\boldsymbol{\theta}}_{S^C} = \mathbf{0}$ and thus to satisfy the KKT condition (16).

To show $\|\mathbf{s}_j\|_2 < 1$, we can solve $\tilde{\boldsymbol{\theta}}_S$ from (15), leveraging the full rank of $\mathbf{G}_S^\top \mathbf{G}_S \in \mathbb{R}^{|S|m \times |S|m}$ from Assumption 4.2, and obtain

$$\tilde{\boldsymbol{\theta}}_S = (\mathbf{G}_S^\top \mathbf{G}_S)^{-1} (\mathbf{G}_S^\top \mathbf{y} - \lambda \mathbf{s}_S)$$

Substituting the formula of $\tilde{\boldsymbol{\theta}}_S$ into (16) and denoting $\mathbf{P}_S := \mathbf{I} - \mathbf{G}_S (\mathbf{G}_S^\top \mathbf{G}_S)^{-1} \mathbf{G}_S^\top$, we get

$$\mathbf{s}_{S^C} = \frac{1}{\lambda} \mathbf{G}_{S^C}^\top \mathbf{P}_S \mathbf{y} + \mathbf{G}_{S^C}^\top \mathbf{G}_S (\mathbf{G}_S^\top \mathbf{G}_S)^{-1} \mathbf{s}_S$$

For $j \notin S$, taking the ℓ_2 norm and applying the triangular inequality give

$$\|\mathbf{s}_j\|_2 \leq \frac{1}{\lambda} \|\mathbf{G}_j^\top \mathbf{P}_S \mathbf{y}\|_2 + \left\| \mathbf{G}_j^\top \mathbf{G}_S (\mathbf{G}_S^\top \mathbf{G}_S)^{-1} \mathbf{s}_S \right\|_2 \quad (17)$$

Applying the Holder's inequality to the second term in (17) gives

$$\left\| \mathbf{G}_j^\top \mathbf{G}_S (\mathbf{G}_S^\top \mathbf{G}_S)^{-1} \mathbf{s}_S \right\|_2 \leq \left\| \mathbf{G}_j^\top \mathbf{G}_S (\mathbf{G}_S^\top \mathbf{G}_S)^{-1} \right\|_2 \|\mathbf{s}_S\|_\infty < 1 - \gamma$$

where the inequality follows from Assumption 4.5 (mutual incoherence).

Regarding the first term in (17), unlike in the LASSO support recovery analysis Wainwright [2009] where the maximal inequality is directly applicable, we seek new tools since $\left\{ \left\| \mathbf{G}_j^\top \mathbf{P}_S \mathbf{y} \right\|_2 \right\}$ are non-centered random variables. We apply the Holder's inequality to the first term in (17),

$$\frac{1}{\lambda} \left\| \mathbf{G}_j^\top \mathbf{P}_S \mathbf{y} \right\|_2 \leq \frac{1}{\lambda} \left\| \mathbf{G}_j^\top \right\|_\infty \left\| \mathbf{P}_S \right\|_2 \left\| \mathbf{y} \right\|_\infty \leq \frac{1}{\lambda} \left\| \mathbf{G}_j^\top \right\|_\infty \left\| \mathbf{y} \right\|_\infty$$

in which the last inequality follows from the fact that \mathbf{P}_S is a projection matrix with $\|\mathbf{P}_S\|_2 \leq 1$.

All in all, we have

$$\max_{j \notin S} \|\mathbf{s}_j\|_2 \leq \frac{1}{\lambda} \max_{j \notin S} \left\| \mathbf{G}_j^\top \right\|_\infty \left\| \mathbf{y} \right\|_\infty + 1 - \gamma$$

and therefore, if $\lambda > \max_{j \notin S} \left\| \mathbf{G}_j^\top \right\|_\infty \left\| \mathbf{y} \right\|_\infty / \gamma$, then SNAM recovers the true support exactly. Notice that the matrix norm $\left\| \mathbf{G}_j^\top \right\|_\infty$ is the maximum of its n absolute value column sums: $\left\| \mathbf{G}_j^\top \right\|_\infty = \max_{i=1}^n \left\| g_j([\mathbf{X}_j]_i, \mathbf{w}_j(0)) \right\|_1$ where $g_j([\mathbf{X}_j]_i, \mathbf{w}_j(0)) \in \mathbb{R}^m$. \square

A.3 Proofs in Section 5

Proof of Theorem 5.1. From Theorem 4.3, we see that $\frac{1}{n} \|f(\mathbf{x}) - h_n(\mathbf{x})\|_2^2 = O_p(1/\sqrt{n}) = o_p(1)$. To prepare the proof of the convergence in probability measure, we consider the probability space consisting of (\mathcal{X}, E, ρ) , where \mathcal{X} is the sample space, E is the event space, and ρ is the probability measure. Defining the events $S_n := \{x \in \mathcal{X} : |f(x) - h_n(x)| \geq \epsilon\}$, we have $S_n \in E$.

We will prove the theorem by contradiction. If there exists an $\epsilon > 0$ such that for any $N, \delta > 0$, there is some $n_N > N$ such that $\rho(\{x \in \mathcal{X} : |f(x) - h_n(x)| \geq \epsilon\}) > \delta$.

However, since

$$\begin{aligned} \frac{1}{n} \|f(\mathbf{x}) - h_n(\mathbf{x})\|_2^2 &= \frac{1}{n} \sum_{i=1}^n (f(\mathbf{x}_i) - h_n(\mathbf{x}_i))_2^2 \\ &\geq \frac{1}{n} \sum_{\mathbf{x}_i \in S_n} (f(\mathbf{x}_i) - h_n(\mathbf{x}_i))_2^2 \\ &= \frac{1}{n} \sum_{i=1}^n \mathbb{I}(\mathbf{x}_i \in S_n) (f(\mathbf{x}_i) - h_n(\mathbf{x}_i))_2^2 \\ &\geq \frac{\epsilon^2}{n} \sum_{i=1}^n \mathbb{I}(\mathbf{x}_i \in S_n) \end{aligned}$$

Denote each random variable $\mathbb{I}(\mathbf{x}_i \in S_n) := Z_{n,i}$. Together they constitute a row-wise i.i.d. triangular array. Since $\sup_n \mathbb{E}(Z_{n,i}^2) \leq 1 < \infty$, by applying the weak law of large number for triangular array [Durrett, 2019, Theorem 2.2.11], we obtain

$$\frac{1}{n} \|f(\mathbf{x}) - h_n(\mathbf{x})\|_2^2 \geq \frac{\epsilon^2}{n} \sum_{i=1}^n \mathbb{I}(\mathbf{x}_i \in S_n) \xrightarrow{P} \epsilon^2 \mathbb{P}(x \in S_n) > \epsilon^2 \delta$$

This contradicts with the asymptotic zero estimation MSE, i.e. $\frac{1}{n} \|f(\mathbf{x}) - h_n(\mathbf{x})\|_2^2 \xrightarrow{P} 0$. \square

Proof of Theorem 5.2. Following the proof of Theorem 5.1, we know for any $\epsilon > 0, \delta > 0$, there exists N such that for any $n_N > N$, we have $\rho(\{x \in \mathcal{X} : |f(x) - h_n(x)| \geq \epsilon\}) < \delta$ and denote $S_n(\epsilon) := \{x \in \mathcal{X} : |f(x) - h_n(x)| \geq \epsilon\}$. We further denote $S_{n,j}^C := \{x_{-j} : (x_j, x_{-j}) \in S_n^C\}$ where S_n^C is the complement of S_n .

Under the condition that \mathcal{X}_j is independent of \mathcal{X}_{-j} , we take the expectation with respect to \mathcal{X}_{-j} , using the marginal density as p_{-j} :

$$\int_{S_{n,j}^C} f(\mathcal{X}) p_{-j}(u) du = \int_{S_{n,j}^C} (f_{n,j}(\mathcal{X}_j) + f_{n,-j}(u)) p_{-j}(u) du = f_{n,j}(\mathcal{X}_j) + c_{j,1}$$

Notice that this integral is also bounded between $\int_{S_{n,j}^C} (h_{n,j}(\mathcal{X}_j) + h_{n,-j}(u) \pm \epsilon) p_{-j}(u) du = \mathbb{P}(\mathcal{X}_{-j} \in S_{n,j}^C)(h_{n,j}(\mathcal{X}_j) \pm \epsilon) + c_{j,2}$. The probability $\mathbb{P}(\mathcal{X}_{-j} \in S_{n,j}^C)$ goes to 1 as $\delta \rightarrow 0$. Further, as $\epsilon \rightarrow 0$, we have $h_{n,j}(\mathcal{X}_j) \xrightarrow{P} f(\mathcal{X}_j) + c_j$ for some constant c_j . \square

B Training SNAM

B.1 Different optimizers

Here we present the detailed optimizers to train the SNAM. Denoting all trainable parameters in all layers of the j -th sub-network as Θ_j , and the loss as $\mathcal{L} + \lambda \sum_j \|\Theta_j\|_2$, then we have

1. Subgradient method:

$$\Theta_j(t+1) = \Theta_j(t) - \eta \left(\frac{\partial \mathcal{L}}{\partial \Theta_j(t)} + \lambda \frac{\Theta_j(t)}{\|\Theta_j(t)\|_2} \cdot 1\{\Theta_j(t) \neq \mathbf{0}\} \right)$$

2. Proximal gradient descent:

$$\Theta_j(t+1) = \text{Prox}_{\lambda\eta} \left(\Theta_j(t) - \eta \frac{\partial \mathcal{L}}{\partial \Theta_j(t)} \right)$$

$$\text{where } \text{Prox}_{\gamma}(x) = \begin{cases} x - \gamma \frac{x}{\|x\|_2}, & x > \gamma \\ 0, & x \leq \gamma \end{cases}$$

Notice that for subgradient methods, we can use Adam, Adagrad, momentum and so on, as long as we set the subgradient of zero vector to be zero. For proximal gradient methods, we can use momentums as well, e.g. in FISTA Beck and Teboulle [2009].

B.2 Different optimization problems

Here we introduce more SNAMs that can perform feature selection using different group penalties.

1. SNAM extended from LASSO (the regular one):

$$\min_{\Theta_j} \mathcal{L} + \lambda \sum_j \|\Theta_j\|_2$$

2. SNAM extended from SLOPE:

$$\min_{\Theta_j} \mathcal{L} + \sum_j \lambda_j (\{\|\Theta_k\|_2\})_{(j)}$$

where $\boldsymbol{\lambda} \in \mathbb{R}^p$ with $\lambda_j > \lambda_{j+1}$, and $(\boldsymbol{v})_{(j)}$ is the j -th largest element in the vector \boldsymbol{v} . I.e. the largest norm is penalized with heaviest penalty.

3. **SNAM extended from 2-level SLOPE:**

$$\min_{\Theta_j} \mathcal{L} + \lambda_1 \sum_{j \leq m} (\{\|\Theta_k\|_2\})_{(j)} + \lambda_2 \sum_{m < j \leq p} (\{\|\Theta_k\|_2\})_{(j)}$$

where λ contains m elements as λ_1 and $p - m$ elements as λ_2 .

4. **SNAM extended from adaptive LASSO:**

$$\min_{\Theta_j} \mathcal{L} + \lambda \sum_j w_j \|\Theta_j\|_2$$

where $w_j \in \mathbb{R}$ is the weight to adjust LASSO's bias. Some suggestions are $w_j = 1/\|\Theta_{j,\text{NAM}}\|_2$ or $1/\|\Theta_{j,\text{SNAM}}\|_2$.

5. **SNAM extended from elastic net:**

$$\min_{\Theta_j} \mathcal{L} + \lambda_1 \sum_j \|\Theta_j\|_2 + \lambda_2 \sum_j \|\Theta_j\|_2^2$$

Note this is regular SNAM with weight decay.

C Figure Zoo

In this section, we show some additional experiments to further verify our conclusions. In Figure 6, Figure 7, and Figure 8, we show the approximation of each methods to the true function. As we mentioned in the main text, all the functions are zero function except the top 4. Since the top 4 functions are non-linear, there is no surprise that ℓ_1 SVM and LASSO have bad performance. For SPAM, although the approximation is better than ℓ_1 SVM and LASSO, it is still beaten by our SNAM, especially in jumpy functions like $f_4(\mathbf{x})$. The models are well tuned and the dataset is the same as in Figure 3. We only show the top 8 figures for simplicity.

The individual effect of different physical quantities to predict the critical temperature of super-conductors

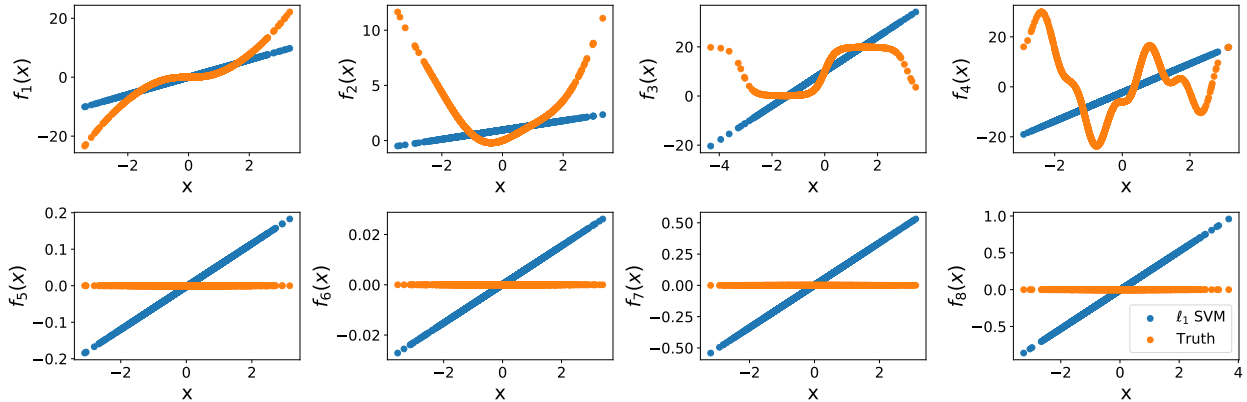


Figure 6: Individual effect learned by ℓ_1 SVM on synthetic regression. Blue dots are prediction $\hat{f}_j(\mathbf{X}_j)$ and orange dots are truth $f_j(\mathbf{X}_j)$, with $j = 1, \dots, 8$.

is demonstrated as below. Features that have small values can be taken as insignificant factors.

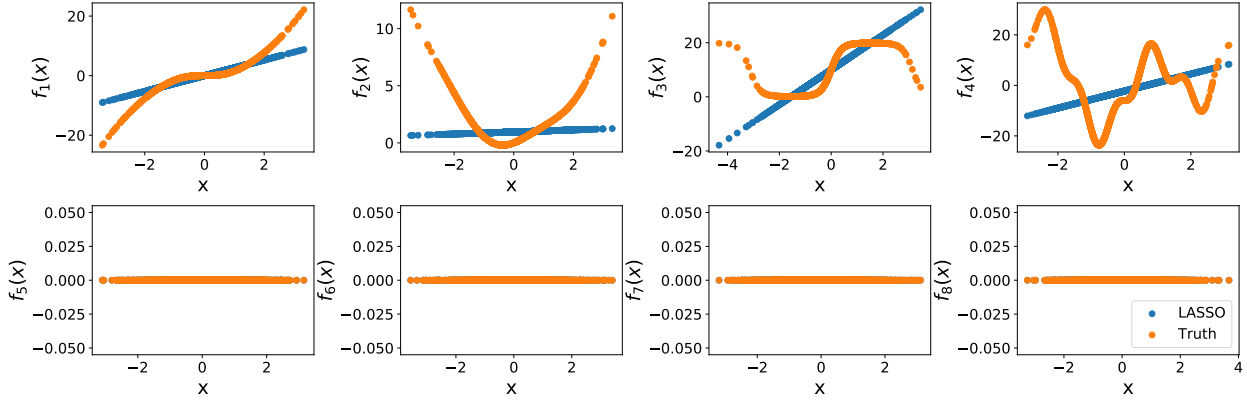


Figure 7: Individual effect learned by LASSO on synthetic regression. Blue dots are prediction $\hat{f}_j(\mathbf{X}_j)$ and orange dots are truth $f_j(\mathbf{X}_j)$, with $j = 1, \dots, 8$.

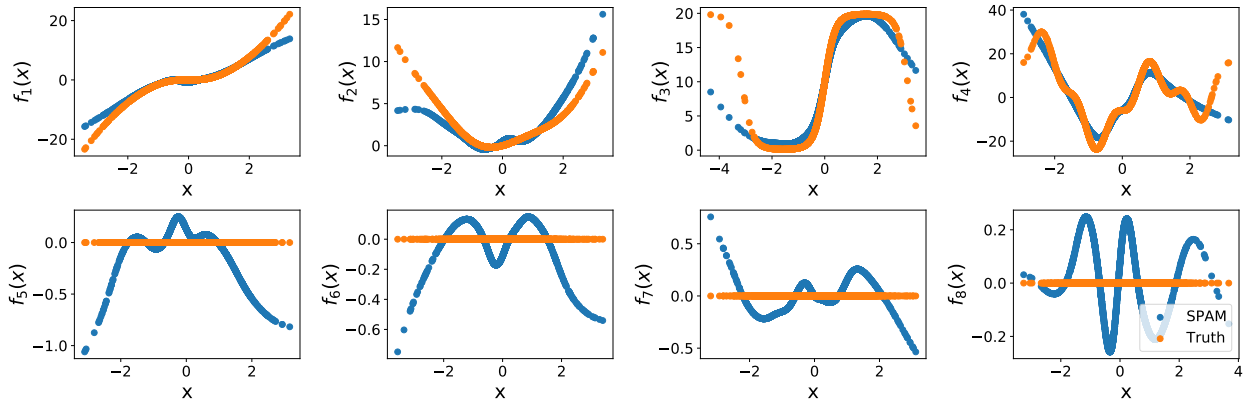


Figure 8: Individual effect learned by SPAM on synthetic regression. Blue dots are prediction $\hat{f}_j(\mathbf{X}_j)$ and orange dots are truth $f_j(\mathbf{X}_j)$, with $j = 1, \dots, 8$.

D Experiment Details

For all the experiments except the one with super-conductivity dataset, we apply the same three-layer architecture for the sub-networks, using ReLU activation. The neurons in the first, the second hidden layers and the output layer are 100, 50, 1 respectively for regression tasks and 100, 50, 2 for binary classification tasks. For the super-conductivity dataset, the sub-networks are two-layer neural networks with 16 hidden neurons for each. Notice that sub-networks have bias terms in hidden layers but not for output layers, since there is a global bias β to be added to the outputs.

The optimizer is Adam by default with batch size 256, except for the super-conductivity dataset, the batch size is 512.

The hyperparameters of SNAM are listed below.

In the experiments over optimizers in Figure 2, we apply the same hyperparameters for Adam, SGD and gradient descent: learning rate is 10^{-6} , penalty is 1 and the number of epoch is 300.

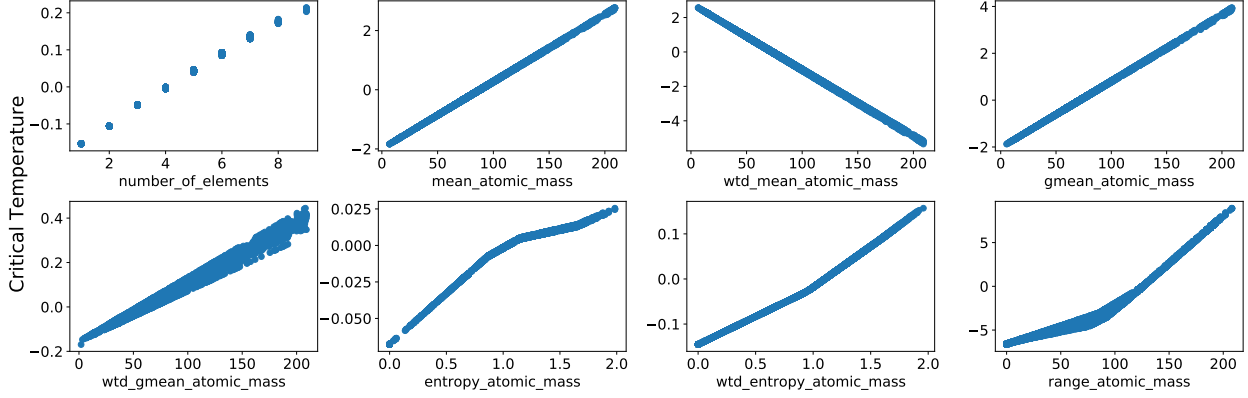


Figure 9: Individual effect learned by SNAM on the super-conductivity dataset.

Hyperparameters	Learning rate	Penalty	Epoch
Synthetic regression	5×10^{-3}	2	100
Synthetic classification	5×10^{-3}	0.04	20
California Housing	10^{-5}	1	300
COMPAS	5×10^{-3}	0.08	100
Super-conductivity	5×10^{-3}	10	20

Table 7: Hyperparameters of experiments.

D.1 Miscellaneous

Algorithm 1 SPAM Backfitting Algorithm

Input Data (\mathbf{X}_i, y_i) , regularization parameter λ .

Initialize $\hat{f}_j = 0$, for $j = 1, \dots, p$

Do until \hat{f}_j converge:

For each $j = 1, \dots, p$:

 (a) Compute the residual: $R_j = \mathbf{y} - \sum_{k \neq j} \hat{f}_k(\mathbf{X}_k)$

 (b) Estimate $P_j = \mathbb{E}[R_j | \mathbf{X}_j]$ by smoothing: $\hat{P}_j = \mathcal{S}_j R_j$

 (c) Estimate norm: $\hat{s}_j^2 = \frac{1}{n} \sum_{i=1}^n \hat{P}_j^2(\mathbf{X}_{ij})$

 (d) Soft-threshold: $\hat{f}_j = [1 - \lambda/\hat{s}_j]_+ \hat{P}_j$

 (e) Center: $\hat{f}_j \leftarrow \hat{f}_j - \sum_{i=1}^n \hat{f}_j(\mathbf{X}_{ij})/n$

Output Individual functions \hat{f}_j
